# Study on phase function in Monte Carlo transmission characteristics of poly-disperse aerosol

**Lu Bai**
**Zhen-sen Wu**
**Shuang-qing Tang**
**Ming Li**
Xidian University
School of Science
Xi'an 710071, China
E-mail: blu@xidian.edu.cn

**Pin-hua Xie**
**Shi-mei Wang**
Chinese Academy of Sciences
Anhui Institute of Optics and Fine Mechanics
Key Laboratory of Environmental Optics
and Technology
Hefei 230031, China

**Abstract.** Henyey–Greenstein (H-G) phase function is typically used as an approximation to Mie phase function and its shortcomings have been discussed in numerous papers. But the judicious criterion of when the H-G phase function would be valid is still ambiguous. In this paper, we use the direct sample phase function method in transmittance calculation. A comparison of the direct sample phase function method and the H-G phase function is presented. The percentage of the multiple scattering in Monte Carlo transfer computations is discussed. Numerical results showed that using H-G phase function led to underestimating the transmittance. The deflection of root means square error can be used as a criterion. Although the exact calculation of sample phase function requires slightly more computation time, the rigorous phase function simulation method has an important role in the Monte Carlo radiative transfer computation problems.
 [DOI: 10.1117/1.3530109]

Subject terms: poly-disperse aerosol; phase function; Monte Carlo.

Paper 100201RRR received Mar. 14, 2010; revised manuscript received Nov. 29, 2010; accepted for publication Nov. 30, 2010; published online Jan. 26, 2011.

## 1 Introduction

There are various methods often used to solve the radiative transfer equations, such as Monte Carlo method, discrete ordinates method, and adding-doubling method, etc. When we examine multiple scattering in aerosol atmospheres using Monte Carlo method, a problem occurs when one simulates the scattering phase function. Approximate phase functions, such as Henyey–Greenstein (H-G), modified Henyey–Greenstein, and Legendre polynomial decomposition, are often used to simulate the Mie phase function.[1–4] These functions are often poor approximations of real phase functions. Toublanc used an exact calculation phase function method and compared Mie phase function with H-G and modified H-G phase functions for mono-disperse particle.[5] Bai et al. simulated real phase function for some typical poly-disperse particle in UV band.[6] Many effective phase functions for light scattered by disperse systems are studied to approximate the real phase functions. However, the judicious criterion of when the HG phase function would be valid is still ambiguous. In this paper, the difference between the two types of phase functionssimulation methods to calculate the transmission rate is presented. The effects of the wavelength, aerosol type, computation time, and the generated random number on Monte Carlo propagation properties are analyzed in the following section.

## 2 Transport Theory of Wave Propagation in Random Particles

According to the radiative transfer equation, the diffuse intensity of incident wave in plane-parallel medium can be expressed as[7]

$$\frac{dI_d(\vec{r},\hat{s})}{ds} = -\rho\sigma_t I_d(\vec{r},\hat{s}) + \frac{\rho\sigma_t}{4\pi}\int_{4\pi} p(\hat{s},\hat{s}')I_d(\vec{r},\hat{s}')d\omega', \quad (1)$$

where $I_d(\vec{r},\hat{s})$ is the diffuse intensity at the point $\vec{r}$ with radiation along the direction $\hat{s}$, $\rho$ is the number density, $d\omega'$ is the solid angle, and $\sigma_t = \sigma_a + \sigma_s$, which is the extinction cross section. $\sigma_a$ and $\sigma_s$ are the absorption and scattering section respectively. Using non-dimensional optical depth $\tau = \int \rho\sigma_t ds$, for plane-parallel atmosphere, Eq. (1) becomes

$$I_d(\bar{\tau},\mu) = \int_0^{\tau_0} \exp\left[-\frac{\bar{\tau}-\tau'}{\mu}\right] J(\tau',\mu)\frac{d\tau'}{|\mu|} + I_{ri}(\bar{\tau},\mu), \quad (2)$$

where

$$J(\tau,\mu) = \frac{1}{2}\int_{-1}^{1} p(\mu,\mu')I_d(\tau,\mu')d\mu' \quad (3)$$

$$\bar{\tau} = \begin{cases} \tau_0 & \mu > 0 \quad I_{ri}(0,\mu) = 0\ (\mu < 0), \\ 0 & \mu < 0 \quad \mu = \cos\theta = \hat{s}\cdot\hat{s}', \end{cases}$$

in which $\theta$ is the scattering angle. Integral Eq. (2) can be expressed as

$$\chi(s) = \sum_{m=0}^{\infty} \chi_m(s), \quad (4)$$

where

$$\chi_m(s) = \int \chi_{m-1}(s_{m-1})K_\chi(s_{m-1}\to s)ds_{m-1} = \int\cdots\int S(s_0)K_\chi(s_0\to s_1)\cdots ds_1 ds_0. \quad (5)$$

Physically, $\chi_m(s)$ in Eq. (5) means the emission density from the source at point $P$, through $m$ times transmission and collision. Thus integral operator $\int K_\chi(s_{l-1}\to s_l)ds_{l-1}$ means that the particle experiences transmission and collision in disperse random medium once. We may rewrite Eq. (5) in

**Table 1** Parameters of particle size distributions of selected disperse media #.

| [a]Aerosol PSD Typical Parameter | | [b]Refractive Indices | | | |
|---|---|---|---|---|---|
| | | Wavelength 300 nm | Wavelength 400 nm | Wavelength 550 nm | Wavelength 694 nm |
| W. A. | $\sigma = 1.09527$ | 1.53, 8E10$^{-3}$ | 1.53, 5E10$^{-3}$ | 1.53,6E10$^{-3}$ | 1.53,7E10$^{-3}$ |
| | $r_m = 0.05\ \mu$m | | | | |
| D. A. | $\sigma = 1.09527$ | 1.53, 8E10$^{-3}$ | 1.53, 8E10$^{-3}$ | 1.53,8E10$^{-3}$ | 1.53, 8E10$^{-3}$ |
| | $r_m = 0.5\ \mu$m | | | | |
| S. A. | $\sigma = 0.69317$ | 1.74,4.7E10$^{-1}$ | 1.74,4.7E10$^{-1}$ | 1.75,4.4E10$^{-1}$ | 1.75,4.3E10$^{-1}$ |
| | $r_m = 0.0118\ \mu$m | | | | |
| O. A. | $\sigma = 0.92028$ | 1.395,5.83E10$^{-7}$ | 1.385,9.90E10$^{-9}$ | 1.381,4.26 E10$^{-9}$ | 1.376,5.04E10$^{-8}$ |
| | $r_m = 0.3\ \mu$m | | | | |

[a]Where W. A., D. A., S. A., and O. A. stand for water soluble aerosol, dust aerosol, soot aerosol and oceanic aerosol respectively.
[b]Data sources of refractive index come from Ref. 10, and aerosol distribution typical parameter come from Ref. 8.

probability model, integral operator $\int K_\chi(s_{l-1} \to s_l)ds_{l-1}$ corresponding to conditional probability $P(s_l\,|s_{l-1}\,)$. Using the statistical estimation method, we may obtain

$$P(s_{l+1}|s_l) = \exp\left[-\sigma_a|(z_{l+1} - z_l)/\cos a_l|\right] \times \eta(h - z_l)\eta(z_l), \tag{6}$$

where $a_l$ is the angle between $l$th photon scattering direction and $z$ axis. Exponential part means photon $l$th scattering probability from point $s_l$ to $s_{l+1}$ without absorption. Analogously, integral operator $\int K_\chi(s_m \to s)ds_m$ corresponding to state transition probability

$$P(s|s_m) = \exp\left[-\sigma_t(h - z_m)/\cos a_m\right]\eta(\cos a_m). \tag{7}$$

Use weight function

$$W_{m+1} = W_m \exp\left[-\sigma_a\,|(z_{m+1} - z_m)/\cos a_m|\right], \tag{8}$$

then, the direct transmission probability $P_0$ is

$$P_0 = W_0 \exp\left[-\sigma_t(h - z_m)/\cos a_0\right]. \tag{9}$$

Each photon is initially assigned a weight $W_0 = 1$, and $a_0$ is the angle between initial incident direction and $z$ axis. Therefore, the statistical estimation of photon transmissivity is

$$P_t = \sum_{m=0}^{\infty} P_m = \sum_{m=0}^{\infty} W_m \exp\left[-\sigma_t(h - z_m)/\cos a_m\right] \times \eta(\cos a_m)\prod_{l=1}^{m}\eta(h - z_l)\eta(z_l), \tag{10}$$

and the statistical estimate of photon reflectivity is

$$P_r = \sum_{m=1}^{\infty} P_m = \sum_{m=1}^{\infty} W_m \exp\left[-\sigma_t(0 - z_m)/\cos a_m\right] \times \eta(-\cos a_m)\prod_{l=1}^{m}\eta(h - z_l)\eta(z_l). \tag{11}$$

When $N$ photons are generated, we may obtain the transmissivity $T$ and the reflectivity $R$

$$T = \frac{1}{N}\sum^{N} P_t, \quad R = \frac{1}{N}\sum^{N} P_r. \tag{12}$$

## 3 Phase Functions of Poly-Disperse Aerosol

The scattering properties of poly-disperse aerosols are subsequently obtained by averaging the single scattering properties of every particle in disperse medium. For uniform isotropic spheres, the average volume optical characteristic is only related to the particle size distribution (PSD) $f\,(r)$, the refractive index $m = n_r + in_{im}$ and the number concentration of particles $n$. The PSD is normalized by the condition $\int_0^\infty f(r)dr = 1$, where $r$ is the radius of a particle. Size distributions of typical aerosol are log- normal distribution[8]

$$f(r) = \frac{1}{\sqrt{2\pi}\sigma r}\exp\left[-\frac{(\ln r - \ln r_m)^2}{2\sigma^2}\right], \tag{13}$$

where $r_m$ and $\sigma$ are the mode radius and standard deviation respectively. Some typical parameters of different aerosols are shown in Table 1. For poly-disperse aerosol, the scattering phase function gives[9]

$$P(\lambda, m, \theta) = \frac{\int_{r_{\min}}^{r_{\max}} p(\lambda, r, m, \theta)\sigma_s(\lambda, r, m)f(r)dr}{\int_{r_{\min}}^{r_{\max}} \sigma_s(\lambda, r, m)f(r)dr}, \tag{14}$$

where $p(\lambda, r, m, \theta)$ is the scattering phase function of a single particle with given size parameter and refractive index.

## 4 Comparison Among Different Phase Function Simulation Methods

Mie scattering phase function is not suitable to solve the radiative transfer function. In addition, it can typically be approximated by the Henyey–Greenstein phase function[11]

$$P_{\mathrm{HG}}(\theta, g) = (1 - g^2)(1 + g^2 - 2g\cos\theta)^{-\frac{3}{2}}, \tag{15}$$

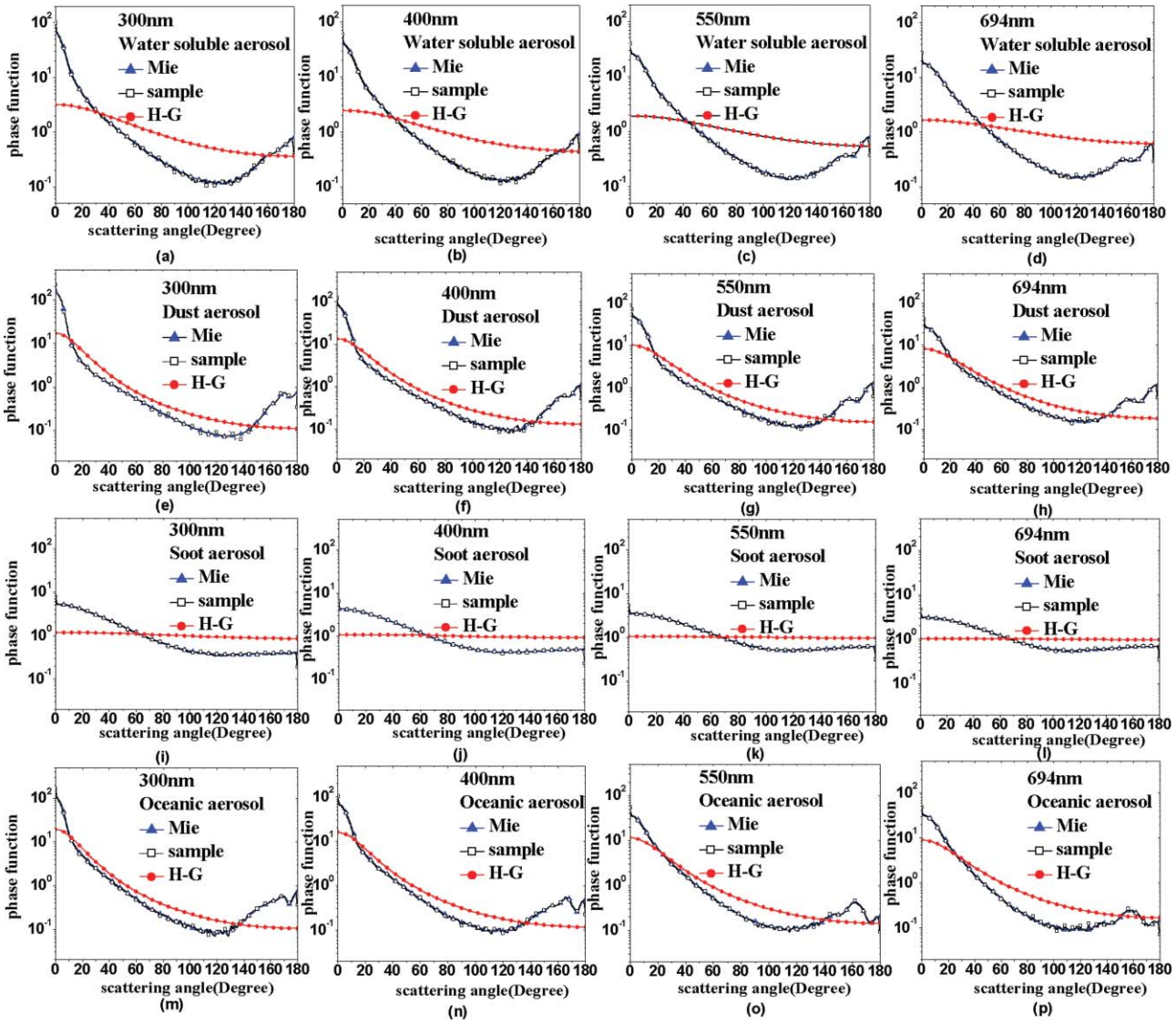


**Fig. 1** Comparison of the phase functions of different simulation methods of aerosol in different incident wavelengths (a)–(d) water soluble aerosol, (e)–(h) dust aerosol, (i)–(l) soot aerosol, and (m)–(p) oceanic aerosol.

$$g = \langle \cos\theta \rangle = \frac{\int p(u)\cos(u)du}{\int p(u)du}, \tag{16}$$

where $g$ is the asymmetry factor. In order to simulate the backscattering behavior, some modified H-G phase functions have been discussed in several articles. Toublanc discussed the H-G and the modified H-G phase functions with a real Mie phase function for single-disperse case with uniform particle radius.[5] We use the direct sample method introduced by Toublanc[5] and Bates[12] to simulate the scattering phase function for poly-disperse case.

**Table 2** Asymmetry parameter *g* averaged with given particle size distributions of aerosol in different wavelength **#.**

| | Asymmetry Parameter *g* | | | |
|---|---|---|---|---|
| Aerosol | Wavelength 300 nm | Wavelength 400 nm | Wavelength 550 nm | Wavelength 694 nm |
| W. A. | 0.3471298 | 0.2759415 | 0.2061835 | 0.1615186 |
| D. A. | 0.6852318 | 0.6487020 | 0.6034039 | 0.5616411 |
| S. A. | 0.0529676 | 0.0299547 | 0.0159331 | 0.0099856 |
| O. A. | 0.7004983 | 0.6737652 | 0.6226931 | 0.5787033 |

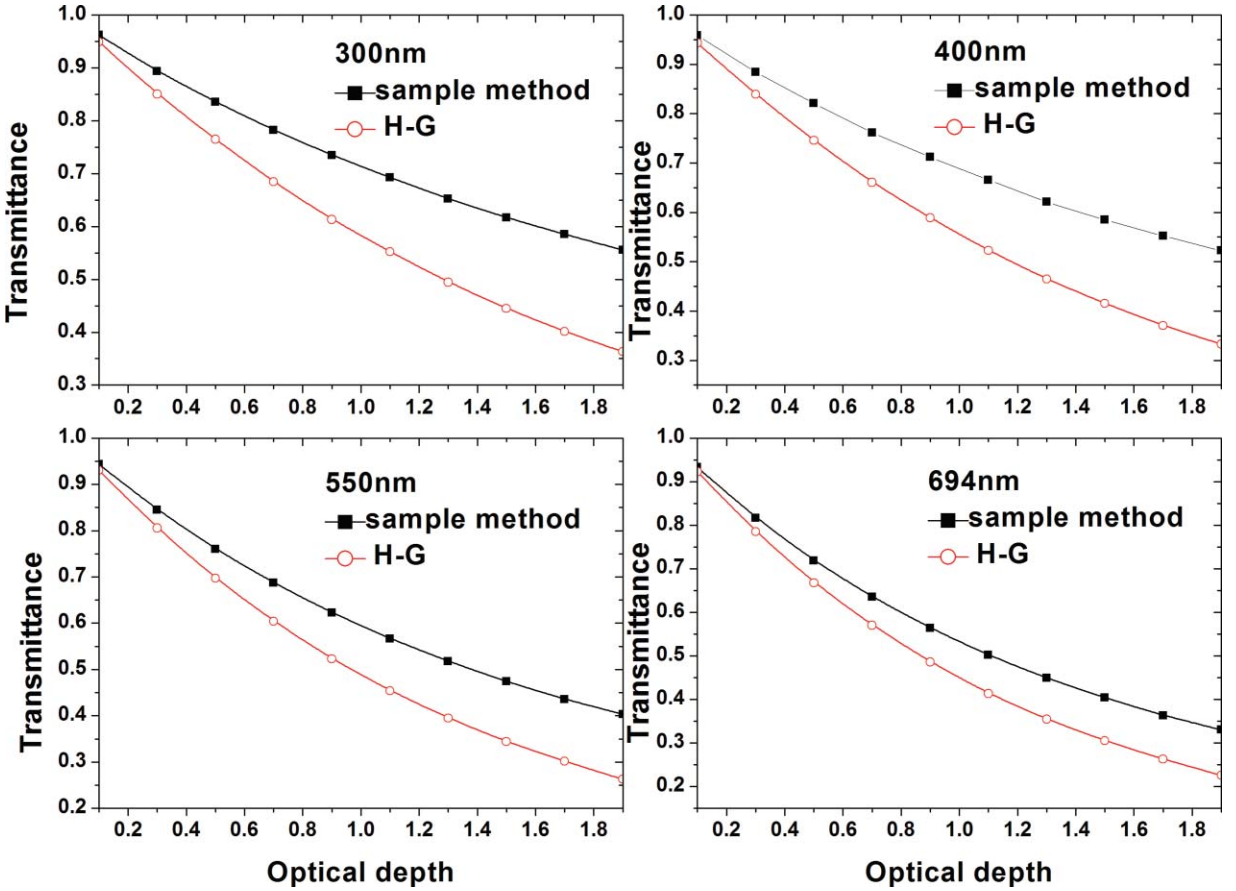


**Fig. 2** Comparison of the transmittance of water soluble aerosol with different scattering phase function simulation methods in different incident wavelength.

This simulation method needs sample random numbers with a given distribution. The random numbers are weighted in a way in which they conform to two basic principles. First, the physical values must be mapped (or scaled) into the range of the RNs (0 to 1). Second, the physical values selected from the RNs must have the same statistical distribution as the naturally occurring distribution. This requires one to develop a cumulative probability distribution lookup table from which mapped values are retrieved.

Our goal is to generate a random number with a uniform distribution between 0 and 1, compare it with the probability distribution, and find the scattering angle corresponding to that number. To do this, a cumulative probability table is developed based on the probability of each scattering angle (namely the scattering phase function). The RN selects a point along the range of probability sums, which then corresponds to a particular scattering angle. Once a RN has been selected, the table is searched until[12]

**Table 3** Root mean square error of selected disperse media with different H-G and random sample simulation method.

| | Wavelength 300 nm | | Wavelength 400 nm | | Wavelength 550 nm | | Wavelength 694 nm | |
|---|---|---|---|---|---|---|---|---|
| Disperse Medium | SM[a] | HG[a] | SM[a] | HG[a] | SM[a] | HG[a] | SM[a] | HG[a] |
| W. A | 2.5150 | 11.0510 | 1.4859 | 7.3944 | 0.9863 | 5.5461 | 0.6855 | 4.2551 |
| D. A | 5.6690 | 20.3627 | 3.1534 | 12.1814 | 1.8309 | 7.6839 | 1.0337 | 4.1861 |
| S. A | 0.1975 | 1.4593 | 0.1617 | 1.2076 | 0.1352 | 0.9929 | 0.1209 | 0.8564 |
| O. A | 4.0660 | 13.8072 | 2.6089 | 9.4424 | 1.3505 | 4.9524 | 1.2110 | 5.1805 |

[a]Where SM and HG stands for random sample method and H-G phase function simulation method respectively.

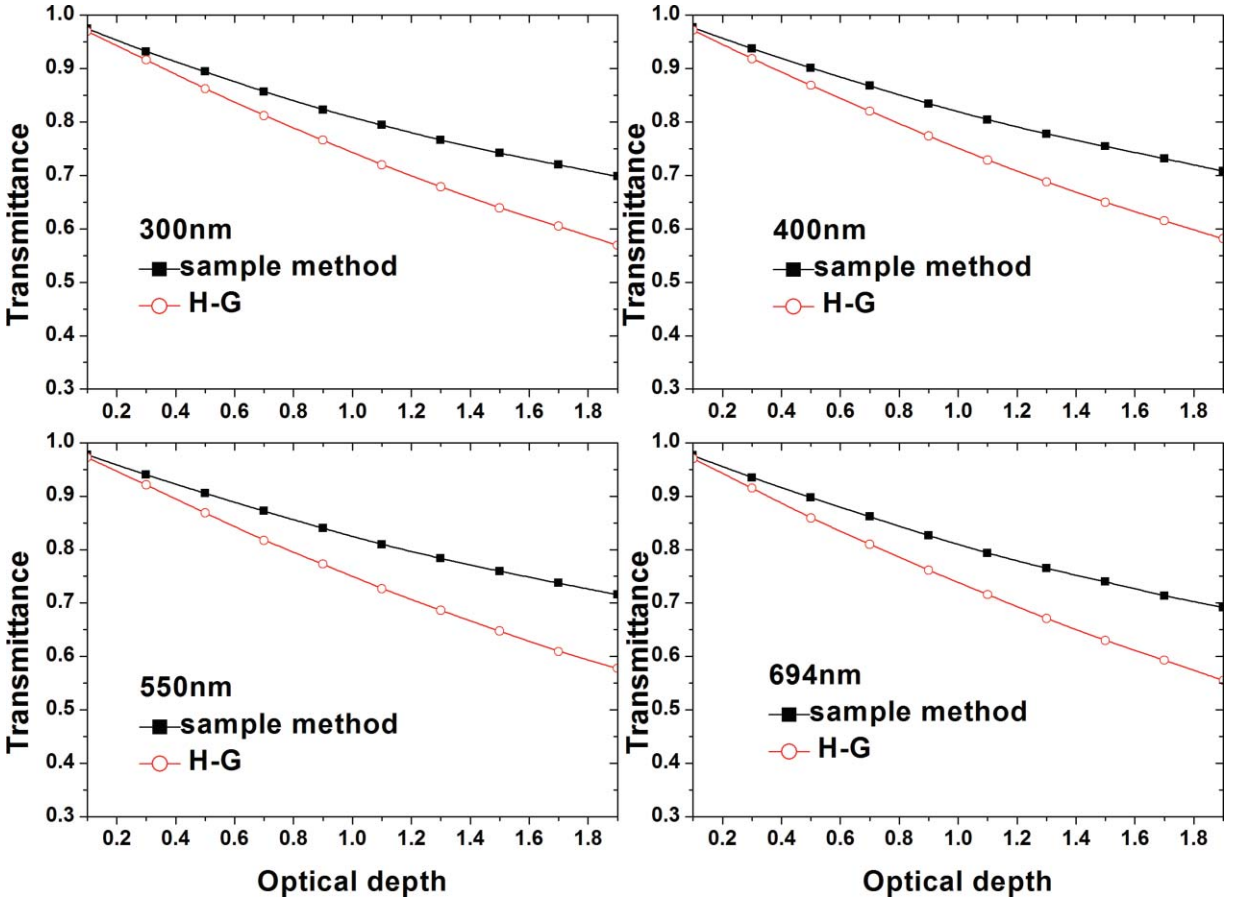


**Fig. 3** Comparison of the transmittance of dust aerosol with different scattering phase function simulation methods in different incident wavelengths.

$$RN = \frac{\sum_0^{\theta_s} p(\theta)\Delta\Omega}{\sum_0^{180} p(\theta)\Delta\Omega}, \tag{17}$$

where $p(\theta)$ is the phase function at scattering angle $\theta$, and $\Delta\Omega$ is the solid angle interval. Using this method the scattering angle $\theta_s$ is selected.

In Fig. 1, we compare the H-G phase functions and the direct sample phase function simulation method with a real Mie phase function intended for four types of poly-disperse aerosol in different incident wavelengths. We choose a 1° step for the phase function and generated 500,000 random numbers.

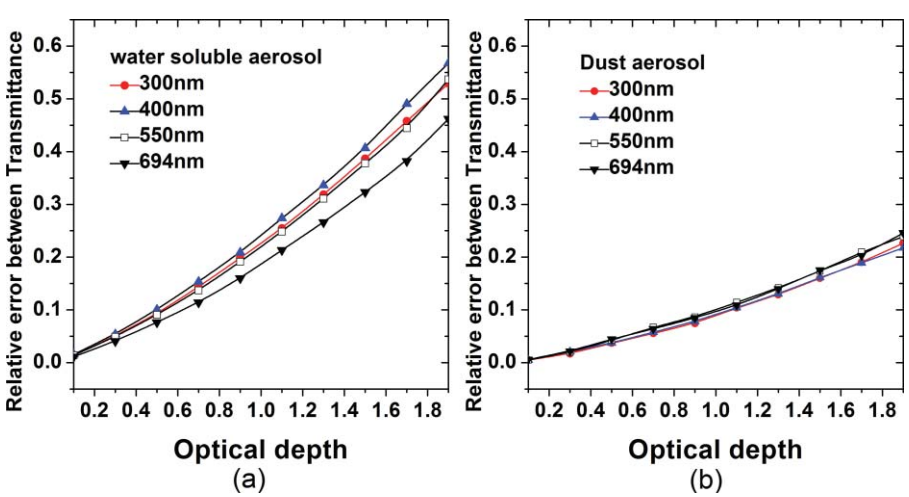


**Fig. 4** Relative error between transmittance of water soluble aerosol and dust aerosol with optical depth in different incident wavelengths.

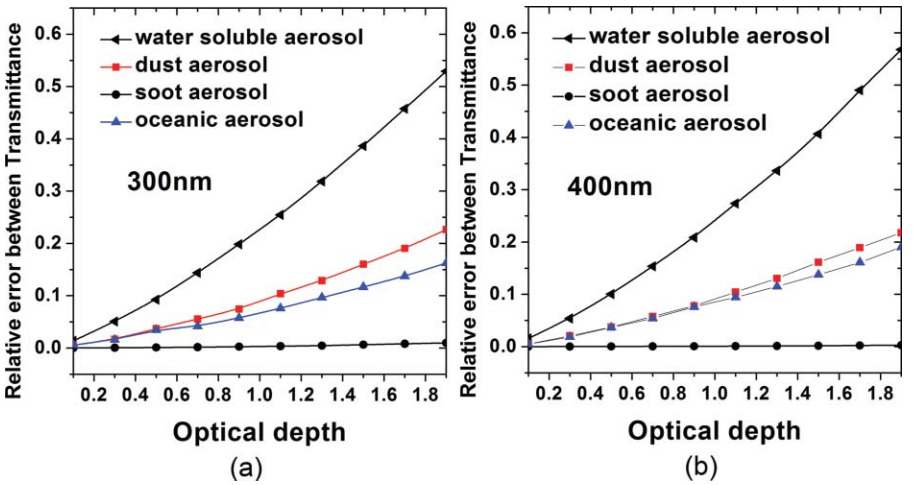


**Fig. 5** Relative error between transmittance of different aerosols with optical depth (a) in 300 nm incident wavelength and (b) in 400 nm incident wavelength.

The asymmetry factor $g$ values for a given particle size distribution (as is showed in Table 1) used in Fig. 1 is presented in Table 2. For given aerosol, the maximum and minimum radius are set to range from 0.01 $\mu$m to 1 $\mu$m.

We notice from Fig. 1 that the difference between Mie scattering phase function and the H-G phase function is obvious. The direct sample method is always better than H-G phase function and closer to Mie results. In order to elucidate the relative difference between these two simulation Mie phase function methods, we introduce root-mean-square error defined as $\sqrt{\{\sum_\theta [p_x(\theta) - p_i(\theta)]^2\}/181}$ where $p_x(\theta)$ is the phase function in scattering angle $\theta$, subscript $x = 1$, 2 means that the phase function simulation method used is H-G or sample method respectively. $p_i(\theta)$ is the poly-disperse aerosol Mie phase function in scattering angle $\theta$.

More attention should be paid, the normalized aerosol phase function is only important in multiple-scattering calculations. In Fig. 1, in order to compare with H-G phase function conveniently, we change the normalized aerosol phase function correspondingly.

In Table 3, comparisons between the root mean square errors of different simulation methods are presented. It is still possible for one to reduce the differences[5] by increasing the number $n$ of random numbers generated since the statistical error decreases as $1/\sqrt{n}$. We observe from the results of Table 3 that the root mean square error of both simulation methods will decrease as the wavelength varies from UV to visible light.

Furthermore, in Table 3, the root mean square error of the sample phase function method could be further reduced by interpolating between the two nearest values in the cumulative probability table, especially in the boundary degrees (0° and 180°) as mentioned briefly in Ref. 12 because the cumulative probability of the phase function changes very fast near these boundary degrees.

In Fig. 2, the plot of the variation of transmittance of water soluble aerosol with optical depth is presented. In Fig. 3, similar results calculated in dust aerosol case are also presented. From Fig. 2 and Fig. 3, we observe that both types of phase function simulation methods will lead to big differences in the calculation of transmittance. Frequently, using H-G phase function simulation method will lead to obviously underestimated results.

As shown in Table 4, the percentage of directly transmittance decreases and the percentage of multiple scattering (photon in collision with aerosol particle two times or more) increases with optical depth increasing. When the optical depth rises to 1.0, the percentage of the multiple scattering increases to 76.497%.

At the same time, the relative error between these two simulation methods varies with wavelength. The transmission curve would be led to larger difference in the UV band, which corresponds to the results shown in Table 3.

In Fig. 4, the relative difference between transmittance of water soluble aerosol and dust aerosol against optical depth in different incident wavelength is presented. Relative difference of transmittance can be defined as $(t_x(\tau)$

**Table 4** Percentage of the directly transmittance, single scattering and multiple-scattering in Monte Carlo transmittance tracing of dust aerosol in 300 nm.

| Optical Depth | Directly Transmittance | Single Scattering | Multiple Scattering |
|---|---|---|---|
| 0.1 | 77.3630 | 18.2832 | 4.35380 |
| 0.2 | 59.9124 | 26.9874 | 13.1002 |
| 0.3 | 46.3260 | 30.4558 | 23.2182 |
| 0.4 | 35.9546 | 30.6302 | 33.4152 |
| 0.5 | 27.6756 | 29.0910 | 43.2334 |
| 0.6 | 21.4484 | 26.5380 | 52.0136 |
| 0.7 | 16.5930 | 23.7622 | 59.6448 |
| 0.8 | 12.8516 | 21.0000 | 66.1484 |
| 0.9 | 9.9302 | 18.2998 | 71.7700 |
| 1.0 | 7.7510 | 15.7520 | 76.4970 |

**Table 5** Comparison of the computation time of different phase function simulation method.

| | W. A. | | | | D. A. | | | | S. A. | | | | O. A. | | | |
|---|---|---|---|---|---|---|---|---|---|---|---|---|---|---|---|---|
| | SM | | HG | | SM | | HG | | SM | | HG | | SM | | HG | |
| Computation time(s) | n1[a] | n2[b] | n1[a] | n2[b] | n1[a] | n2[b] | n1[a] | n2[b] | n1[a] | n2[b] | n1[a] | n2[b] | n1[a] | n2[b] | n1[a] | n2[b] |
| 300 nm | 2 | 18 | 1 | 9 | 1 | 18 | 1 | 9 | 0.4 | 3 | 1 | 1 | 2 | 22 | 1 | 10 |
| 400 nm | 2 | 18 | 1 | 9 | 2 | 19 | 1 | 9 | 0.4 | 2 | 0.4 | 1 | 2 | 22 | 1 | 10 |
| 550 nm | 2 | 18 | 1 | 7 | 2 | 21 | 1 | 9 | 1 | 2 | 1 | 1 | 2 | 22 | 1 | 10 |
| 694 nm | 2 | 14 | 1 | 7 | 2 | 21 | 1 | 10 | 0.4 | 1 | 0.4 | 1 | 2 | 23 | 2 | 11 |

[a]n1 stands for 50,000 random numbers generated.
[b]n2 stands for 500,000 random numbers generated. And the computation time is in second.

$-t_{\mathrm{HG}}(\tau))/t_{\mathrm{HG}}(\tau)$, where $t_x(\tau)$ and $t_{\mathrm{HG}}(\tau)$ stand for transmittance calculation results obtained from sample method or H-G phase function simulation method respectively. Figure 4 leads us to the conclusion that the relative difference of transmittance will increase with the optical depth. Furthermore, the relative difference of transmittance between these two phase function simulation methods change from 1% to 20% when the aerosol optical depth varies from 0.1 to 1.0.

The relative difference of transmittance versus with different kinds of aerosol in 300 nm or 400 nm is presented in Fig. 5. Soot aerosol has the smallest difference between these two types of phase function simulation methods. Its physical explanation suggests that soot aerosol has the smallest albedo and the asymmetry parameter among the four types of aerosols, as is displayed in Table 2. Small albedo and asymmetry parameter means the scattering is isotropy. In this case, using H-G phase function simulation method is a sufficient approximation. In addition, the root-mean-square error of soot aerosol is the smallest, as is displayed in Table 3.

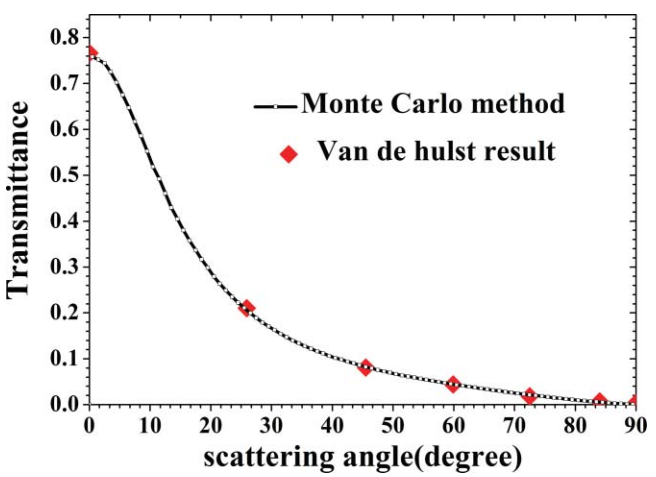


**Fig. 6** Angularly resolved transmittance vs angle between the photon exiting direction and the normal to the medium surface angle. Red solid circles are results from van de Hulst's table, and the black line with white hole is from our Monte Carlo simulation results. (also see Fig. 6.2 in Ref. 14).

Table 5 shows a summary of the results of computation time between sample phase function simulation method (SM) and H-G phase function simulation method (HG). When the random number generated in the sample method is 50,000, SM almost costs twice the computation time compared with the HG phase function simulation method. When the generated random number increases to 500,000, both the SM and the HG will cost more time, and SM will still cost twice or triple computation time than H-G phase function simulation method. But, all of the computation time is in second unit and it can be tolerant.

To test our Monte Carlo results, we compare our results with Refs. 13 and 14. The transmittance versus angle between the photon exiting direction and the normal to the medium surface angle are presented in Fig. 6 red solid circles result from van de Hulst's table and the black line with white hole is from our simulation results (also see Fig. 6.2 in Ref. 14). The parameter shown in the calculation of Fig. 6 is particle radius $d = 0.02\,\mathrm{cm}$. Scattering coefficients is $\mu_s = 90\,\mathrm{cm}^{-1}$. Absorption coefficient is $\mu_a = 10\,\mathrm{cm}^{-1}$. The asymmetry factor is $g = 0.75$ and the albedo is $\omega_0 = 0.9$. The calculated results agree with the Refs. 13 and 14 well.

## 5 Conclusions

The phase function is an important parameter that affects the distribution of scattered radiation. When the Henyey–Greenstein approximation phase function is applied to different kinds of aerosol, it produces a significant difference in transmittance calculations. In this paper, we discussed the applicability criterion of the Henyey–Greenstein approximation phase function method. When the scattering close to isotropy and the root mean square error is small enough, the Henyey–Greenstein approximation phase function simulation method provides adequate results. Besides, although the direct sample phase function method costs a little more computation time, it still should be considered.

### *Acknowledgments*

This work was funded by the National Natural Science Foundation of China (Grant Nos. 60971065 and 60771038) and the Fundamental Research Funds for the Central Universities.

## References


1. L. Reynolds and N. J. McCormick, "Approximate two-parameter phase function for Light Scattering," *J. Opt. Soc. Am.* **70**(10), 1206–1212 (1980).
2. Q. Liu and F. Weng, "Combined Henyey–Greenstein and Rayleigh phase function," *Appl. Opt.* **45**(28), 7475–7479 (2006).
3. I. Turcu, "Effective phase function for light scattered by blood," *Appl. Opt.* **45**(4), 639–647 (2006).
4. W. Fowler, "Expansion of Mie-theory phase functions in series of Legendre polynomials," *J. Opt. Soc. Am.* **73**(1), 19–22 (1983).
5. Toublanc, "Henyey–Greenstein and Mie phase functions in Monte Carlo radiative transfer computations," *Appl. Opt.* **35**(18), 3270–3274 (1996).
6. L. Bai, S. Q. Tang, Z. S. Wu, P. H. Xie, and S. M. Wang, "Study of random sample scattering phase functions of polydisperse atmospheric aerosol in ultraviolet band," *Acta Phys. Sin.* **59**(03), 1749–1755 (2010).
7. A. Ishimaru, *Wave Propagation and Scattering in Random Media*, Academic, New York (1978).
8. A. Kokhanovsky, *Light Scattering Media Optics: Problems and Solutions*, Praxis-Springer, Chichester (2001).
9. E. J. McCartney, *Optics of the Atmosphere*, Beijing: Science Press, (in Chinese) (1988).
10. C. Levoni, M. Cervino, R. Guzzi, and F. Torricella, "Atmospheric aerosol optical properties: a database of radiative characteristics for different components and classes," *Appl. Opt.* **36**(30), 8031–8041 (1997).
11. L. C. Henyey and J. L. Greenstein, "Diffuse radiation in the galaxy," *Astrophys. J.* **93**, 70–83 (1941).
12. D. E. Bates and J. N. Porter, "AO3D: A Monte Carlo code for modeling of environmental light propagation," *J. Quant. Spectrosc. Radiat. Transf.* **109**, 1802–1814 (2008).
13. H. C. Van de Hulst, *Multiple Light Scattering, Tables, Formulas, and Applications*, Academic, New York (1980).
14. L. H. Wang, "Monte Carlo modeling of light transport in multi-layered tissues in standard C," PhD Thesis, Texas A&M University, 1998; http://biomed.tamu.edu/~lw.


Biographies and photographs of the authors not available.